Root-specific activation of plasma membrane H^+-ATPase 1 enhances plant growth and shoot accumulation of nutrient elements under nutrient-poor conditions in *Arabidopsis thaliana*

Kota Monden[a], Takehiro Kamiya[b], Daisuke Sugiura[c], Takamasa Suzuki[d], Tsuyoshi Nakagawa[a] and Takushi Hachiya[a†]

[a]Department of Molecular and Functional Genomics, Interdisciplinary Center for Science Research, Shimane University, Matsue 690-8504, Japan

[b]Graduate School of Agricultural and Life Sciences, The University of Tokyo, Tokyo 113-8657, Japan

[c]Graduate School of Bioagricultural Sciences, Nagoya University, Nagoya 464-8601, Japan

[d]College of Bioscience and Biotechnology, Chubu University, Kasugai 487-8501, Japan

[†]To whom correspondence should be addressed.

E-mail: takushi.hachiya@life.shimane-u.ac.jp

Tel.: +81-852-32-6288

Fax: +81-852-32-6109

Abbreviations: GO, Gene Ontology; NUE, Nutrient uptake efficiency; PCA, Principal component analysis; PM, plasma membrane; RPM, Reads per million mapped reads; RT, Reverse transcription; SA, Salicylic acid; SAR, Systemic acquired resistance; WT, Wild-type

Abstract

Plasma membrane (PM) H^+-ATPase contributes to nutrient uptake and stomatal opening by creating proton gradient across the membrane. Previous studies report that a dominant mutation in the *OPEN STOMATA2* locus (*OST2-2D*) constitutively activates *Arabidopsis* PM H^+-ATPase 1 (AHA1), which enlarges proton motive force for root nutrient uptake. However, the stomatal opening is also constitutively enhanced in the *ost2-2D*, causing the drought hypersensitivity. To develop a plant whose nutrient uptake is improved with normal stomatal movement, we generated grafted plants (scion/rootstock : Col-0 (WT)/*ost2-2D*), and compared their growth and ionome profile with those of control plants (WT/WT) under nutrient-rich or nutrient-poor conditions. WT/*ost2-2D* shoots had larger fresh weight, dry weight, rosette diameter, leaf blade area, and contents of C, N, K, Ca, S, P, Mg, Na, Mn, B, Co, and Mo under nutrient-poor conditions compared with WT/WT shoots. The root fresh and dry weights and primary root length were greater in WT/*ost2-2D* roots than in WT/WT roots under both nutrient conditions. These results suggest that root-specific activation of PM H^+-ATPase enhances root nutrient uptake, which accelerates the plant growth under nutrient-poor condition. Our study presents a novel approach to improving nutrient uptake efficiency in crops and vegetables; thus, it could contribute to the implementation of low-input sustainable agriculture.

Keywords: *Arabidopsis thaliana*; micrografting; nutrient uptake efficiency; OPEN STOMATA 2; plasma membrane H^+-ATPase

46 **1. Introduction**

47 As the global population increases, crop production must also increase. Nutrient availability is an
48 important determinant of crop productivity; thus, fertilizers are often applied in large amounts to
49 improve crop production. Intensive fertilizer use, however, puts a heavy burden on the environment,
50 e.g., through groundwater pollution, eutrophication, and greenhouse gas emissions [1]. N, P, and K,
51 macronutrients typically in high demand in plants, account for a major portion of applied fertilizers.
52 The artificial synthesis of N fertilizers requires massive fossil fuel consumption; i.e., ammonia
53 synthesis via the Harber–Bosch process consumes 1%–2% of the global energy budget currently [2].
54 Additionally, the P contained in fertilizers is derived from nonrenewable rock phosphate that will be
55 depleted in the future [3]. Thus, developing plants with high nutrient uptake efficiency (NUE) is
56 crucial to achieving sustainable agriculture.

57 It is widely accepted that plasma membrane (PM) H^+-ATPase provides proton motive force
58 for root nutrient uptake mediated by specific transporters and channels [4]. Constitutive
59 overexpression of *Oryza sativa* PM H^+-ATPase 1 (*OSA1*) under the control of the *CaMV-35S* promoter
60 was shown to enhance root uptake of ammonium, plant growth, and productivity in both the field and
61 laboratory [5]. Conversely, similar overexpression of PM H^+-ATPase genes failed to confer any
62 positive effects on *Arabidopsis* and tobacco plants [6, 7]. Importantly, post-translational activation of
63 PM H^+-ATPase often has major effects on *Arabidopsis* physiological responses, including stomatal
64 opening and hypocotyl elongation [8, 9]. Therefore, with the aim of improving the NUE of
65 *Arabidopsis*, we focused on the *Arabidopsis OPEN STOMATA 2* (*OST2*)-dominant mutant (*ost2-2D*),
66 which expresses a constitutively active allele of the *Arabidopsis* PM H^+-ATPase 1 (*AHA1*) [9]. This
67 mutant exhibits lower apoplastic pH and longer-sized root epidermal cells, corresponding to
68 enhancements in proton motive force and acid growth in the roots, respectively [10]. However, PM
69 hyperpolarization in the guard cells of *ost2-2D* causes drought hypersensitivity due to the prevention
70 of stomatal closure, even with the addition of abscisic acid [9, 11, 12]. Thus, the root-specific
71 activation of OST2/AHA1 could be an ideal design for improving NUE. To achieve this design, we
72 grafted Col-0 (wild-type; WT) scions onto rootstock originating from WT or *ost2-2D* and analyzed

73 the vegetative growth, nutrient element content, and transcriptomes of the grafted plants grown under
74 nutrient-rich or nutrient-poor conditions. We show that *ost2-2D*-derived rootstock enhances the
75 growth of shoots and roots as well as the shoot accumulation of several nutrient elements under
76 nutrient-poor conditions.

77

78 **2. Materials and methods**

79 *2.1. Plant materials and growth conditions*

80 Seeds of Col-0 (WT) and *ost2-2D* [9] were surface sterilized and sown in a solid medium containing
81 50 mL of half-strength Murashige and Skoog (1/2-MS) salts including vitamins (Code M0222;
82 Duchefa Biochemie, Haarlem, The Netherlands) supplemented with 0.05% (w/v) MES-KOH (pH 5.7),
83 1% (w/v) sucrose, and 0.5% (w/v) gellan gum (Fujifilm Wako, Osaka, Japan). The seeds were placed
84 in the dark at 4°C for 3 days to break dormancy. Seedlings were grown vertically under a PPFD of
85 25 μmol m^{-2} s^{-1} (16/8-h light/dark cycle) at 22°C. Micrografting was performed aseptically using 5-
86 day-old seedlings [13], which were cut perpendicularly in the hypocotyl with an injection needle tip
87 (Code NN-2613S; TERUMO, Tokyo, Japan). The obtained scion was connected with the partner
88 rootstock in a silicon microtube (Code 1-8194-04; AS ONE, Osaka, Japan). The grafted plants were
89 incubated for 5 days under a PPDF of 50 μmol m^{-2} s^{-1} (constant light) at 27°C and further cultivated
90 for a few days under a PPFD of 25 μmol m^{-2} s^{-1} (16/8-h light/dark cycle) at 22°C. Successfully grafted
91 plants without adventitious root formation were selected for similar size; transferred to vermiculite
92 pots, soil pots, or solid media; and grown for use in the following experiments. For vermiculite
93 cultivation, the grafted plants were grown under a PPFD of 100–120 μmol m^{-2} s^{-1} (16/8-h light/dark
94 cycle) at 22°C–23°C. Before the cultivation, ~150 mL of vermiculite was soaked with 80 mL of 1/2-
95 MS or 1/50-MS salts without vitamins (Code M0221; Duchefa Biochemie) supplemented with 0.05%
96 (w/v) MES-KOH (pH 5.7). Four days after the onset of cultivation, 30 mL of the same compositions
97 of 1/2-MS or 1/50-MS salts was supplied to the vermiculite. The plants were then cultivated for an
98 additional 3 days; after which, they were sampled for experiments. For soil cultivation, the grafted

99 plants were grown for 7 days under a PPFD of 100–120 μmol m^{-2} s^{-1} (16/8-h light/dark cycle) at
100 22°C–23°C in the pots containing ~150 mL of nutrient-rich soil (Supermix A; Sakata Seed, Kyoto,
101 Japan). For an *in vitro* culture on solid media, the plants were grown for 3 days (vertically) or 7 days
102 (horizontally) under a PPFD of 100–120 μmol m^{-2} s^{-1} (16/8-h light/dark cycle) at 22°C–23°C in
103 30 mL (horizontally) or 50 mL (vertically) of 1/2-MS or 1/50-MS salts without vitamins (Duchefa
104 Biochemie) supplemented with 0.05% (w/v) MES-KOH (pH 5.7), 1% (w/v) sucrose, and 0.8% (w/v)
105 purified agar (Code 01162-15; Nacalai Tesque, Kyoto, Japan). To allow nondestructive sampling of
106 the roots, the surfaces of solid media were covered with cellophane sheets [14]. All other details are
107 described in the figure legends.
108
109 *2.2. Growth analysis of plants under vermiculite and soil cultivation*
110 Shoots were weighed on a precision balance (HR-202i; A&D, Tokyo, Japan) and scanned at a
111 resolution of 600 dpi (GT-X980; EPSON, Tokyo, Japan) to measure rosette diameter. Leaf blades
112 were harvested from the shoots and scanned at a resolution of 600 dpi to measure the area of the leaf
113 blades. The shoots were then oven-dried at 80°C for 2 days and recovered in a desiccator with silica
114 gel. Shoot dry weights were measured using the precision balance, and the rosette diameter and leaf
115 blade area were measured using ImageJ version 1.52p.
116
117 *2.3. Growth analysis of plants under* in vitro *culture on solid media*
118 The shoots and roots of horizontally grown plants were weighed using the precision balance, after
119 which they were oven-dried at 80°C for 2 days and recovered in a desiccator with silica gel. The dry
120 weights of the shoots and roots were measured using the precision balance. The roots of vertically
121 grown plants were scanned at a resolution of 600 dpi to measure the length and number of primary
122 and lateral roots (>0.3 mm). Root length was measured using ImageJ version 1.52p.
123
124 *2.4. Determination of nutrient elements*

125 Harvested shoots were oven-dried at 80°C for 2 days, and the dried samples were ground using a spoon
126 and recovered in a desiccator with silica gel. For determination of C and N, the dried powder was
127 weighed and encapsulated in a tin boat, and C and N concentrations were measured using a CN
128 analyzer (Vario EL III; Elementar Analysensysteme GmbH, Hanau, Germany). For determination of
129 K, P, S, Ca, Fe, Mg, Mn, Na, B, Co, Cu, Mo, and Zn, the dried samples were weighed and digested
130 using 2 mL of concentrated HNO_3 followed by the addition of 1 mL of H_2O_2 at 120°C until it
131 evaporated. The digested samples were dissolved in 0.08 M HNO_3 and the element concentrations
132 were measured using inductively coupled plasma–mass spectrometry (Agilent 7800 ICP-MS; Agilent
133 Technologies, Santa Clara, CA, USA) using 2 ppb indium as an internal standard.
134
135 *2.5. Extraction of total RNA*
136 Roots were harvested, immediately frozen using liquid N_2, and stored at −80°C until use. Frozen
137 samples were ground with a Multi-Beads Shocker (Yasui Kikai, Osaka, Japan) using zirconia beads
138 (diameter: 5 mm). Total RNA was extracted using an RNeasy Plant Mini Kit (Qiagen, Tokyo, Japan)
139 according to the manufacturer's instructions. For RNA-Seq library preparation, RNA was purified
140 using on-column DNase digestion (Qiagen).
141
142 *2.6. RT-qPCR*
143 Reverse transcription (RT) was performed using ReverTra Ace qPCR RT Master Mix with gDNA
144 Remover (Toyobo, Osaka Japan) according to the manufacturer's instructions. The synthesized cDNA
145 was diluted 10-fold with distilled water and used in quantitative PCR (qPCR). RT-qPCR was
146 performed on a QuantStudio 1 (Thermo Fisher Scientific) with KOD SYBR qPCR Mix (Toyobo)
147 according to the manufacturer's instructions. Transcript levels were quantified using a relative standard
148 curve with *ACTIN3* as the internal standard [19]. Primer sequences are shown in Supplementary Table
149 1.
150
151 *2.7. RNA-Seq analysis*

152 RNA quality was evaluated using a Qubit RNA IQ Assay Kit with a Qubit 4 Fluorometer (Thermo
153 Fisher Scientific, Tokyo, Japan). The RNA samples for which RNA IQs were 9.1–10.0 were used for
154 the following preparation. cDNA libraries were constructed using a NEBNext Ultra II RNA Library
155 Prep with Sample Purification Beads (Code E7775; New England Biolabs, Tokyo, Japan), a NEBNext
156 Poly(A) mRNA Magnetic Isolation Module (Code E7490; New England Biolabs), and a NEBNext
157 Multiplex Oligos for Illumina (Index Primers Set 3) (Code E7710; New England Biolabs) according
158 to the manufacturer's instructions. These cDNA libraries were sequenced using NextSeq 500 (Illumina,
159 Tokyo, Japan), and the produced bcl files were converted to fastq files using bcl2fastq (Illumina). The
160 obtained reads were analyzed according to the method described by Notaguchi et al. [15] and mapped
161 to the *Arabidopsis* reference (TAIR10) using Bowtie [16] with the following options: "--all --best --
162 strata." The number of reads mapped to each reference was counted, and the total read counts of splice
163 variants from a gene were used for further analysis via the iDEP ver. 095 integrated web application
164 [17] with the default settings. Pathway analysis was performed using the Metascape web application
165 [18]. Information about read counts is provided in Supplementary Table 2.
166
167 *2.8. Statistical analysis*
168 Unpaired two-tailed Welch's *t*-tests were conducted using R v.2.15.3.
169
170 **3. Results**
171 *3.1. Confirmation of root-specific missense mutation of OST2/AHA1*
172 To manipulate the activity of OST2/AHA1 in a root-specific manner, we grafted WT scions onto
173 rootstock originating from WT or *ost2-2D* (Supplementary Fig. 1A). To confirm the missense
174 mutation (G867S) of *OST2*/*AHA1* reported previously [9], we extracted RNA from the shoots and
175 roots of grafted plants (scion/rootstock: WT/WT and WT/*ost2-2D*). RT-PCR was performed using
176 primers specific to *OST2*/*AHA1*; after which, the PCR products were sequenced directly. The missense
177 mutation was detected only in the cDNA derived from the WT/*ost2-2D* roots (Supplementary Fig. 1B).

178

179 *3.2. Root-specific activation of OST2/AHA1 enhances shoot growth under nutrient-poor conditions*

180 Grafted plants were transferred to vermiculite pots to analyze the effects of root-specific activation of
181 OST2/AHA1 on shoot growth. Following cultivation for 7 days under nutrient-rich (1/2-MS salts) or
182 nutrient-poor conditions (1/50-MS salts), shoot growth was analyzed. WT/*ost2-2D* plants exhibited
183 increased shoot growth relative to that of WT/WT plants under 1/50-MS but not 1/2-MS conditions
184 (Fig. 1A). Under 1/50-MS conditions, shoot fresh and dry weights were significantly increased by
185 28% and 31%, respectively, in WT/*ost2-2D* plants than in WT/WT plants (Fig. 1A). Additionally,
186 rosette diameter and leaf blade area were significantly increased by 13% and 29%, respectively, in
187 WT/*ost2-2D* plants than in WT/WT plants under 1/50-MS conditions (Fig. 1A). Under 1/2-MS
188 conditions, however, only the shoot dry weight was significantly increased by 11% in WT/*ost2-2D*
189 plants (Fig. 1A). When the grafted plants were grown in pots containing nutrient-rich soil or in solid
190 media containing 1/2-MS or 1/50-MS, the shoot fresh and dry weights, rosette diameter, and leaf blade
191 area in WT/*ost2-2D* plants were slightly, albeit not always significantly, increased compared with
192 those in WT/WT plants (Supplementary Fig. 2A, B). Relative water contents of shoots did not
193 substantially decrease in WT/*ost2-2D* plants compared with those in WT/WT plants regardless of
194 nutritional availability and cultivation style (Supplementary Fig. 3A–C). Thus, root-specific activation
195 of OST2/AHA1 does not cause shoot desiccation due to excessive stomatal opening.

196

197 *3.3. Root-specific activation of OST2/AHA1 enhances root growth irrespective of nutrient availability*

198 Barbez et al. [10] reported that the epidermal cell length of the primary roots of *ost2-2D* seedlings is
199 significantly larger than that of WT plants, suggesting that root growth is altered because of root-
200 specific activation of OST2/AHA1. To confirm this, the root growth of grafted plants grown vertically
201 on solid media containing 1/2-MS or 1/50-MS salts was analyzed. The appearance of the roots in
202 WT/WT plants differed according to nutrient condition, and their fresh and dry weights and lateral
203 root length were generally increased under 1/50-MS conditions than under 1/2-MS conditions (Fig.
204 1B and Supplementary Fig. 4A). In WT/*ost2-2D* plants relative to in WT/WT plants, root fresh weight

205 and root dry weight were significantly increased by 30% and 41% under 1/2-MS conditions,
206 respectively, and by 28% and 23% under 1/50-MS conditions, respectively (Fig. 1B). The primary
207 root length was significantly increased in WT/*ost2-2D* plants by 22% and 32% under 1/2-MS and
208 1/50-MS conditions, respectively; however, no significant difference was observed in the lateral root
209 length of the grafted plants (Fig. 1B). In grafted plants grown horizontally on solid media, root fresh
210 and dry weights were increased in WT/*ost2-2D* plants than in WT/WT plants irrespective of nutrient
211 availability (Supplementary Fig. 4B).
212
213 *3.4. Root-specific activation of OST2/AHA1 increases the shoot content of nutrient elements*
214 Zhang et al. [5] reported that constitutive overexpression of *OSA1* significantly increases the content
215 of C, N, K, P, and Ca in the leaves of rice grown in nutrient-rich hydroponic solution. Thus, we
216 determined the content of C and the 14 nutrient elements contained in MS salts in the shoots of grafted
217 plants grown in vermiculite. The content of C, N, K, Ca, S, P, Mg, Na, Mn, B, Co, and Mo was
218 significantly increased in WT/*ost2-2D* shoots than in WT/WT shoots under 1/50-MS conditions (Fig.
219 2). In particular, the content of macronutrients N, K, Ca, S, and P was consistently increased by 54%,
220 37%, 24%, 31%, and 44%, respectively, in WT/*ost2-2D* shoots than in WT/WT shoots (Fig. 2). Under
221 1/2-MS conditions, however, only Na content was significantly increased in the WT/*ost2-2D* shoots
222 than in the WT/WT shoots, although several elements showed increasing trends in the WT/*ost2-2D*
223 shoots (Fig. 2). The shoot concentrations of nutrient elements were generally comparable between the
224 grafted plants regardless of nutrient availability (Supplementary Fig. 5).
225
226 *3.5. Root-specific activation of OST2/AHA1 alters root expression of genes related to biotic responses*
227 To explore the effects of root-specific activation of *OST2/AHA1* on the root transcriptome, we
228 performed RNA-Seq analysis on the roots of grafted plants grown horizontally on solid media
229 containing 1/2-MS or 1/50-MS salts. Hierarchical clustering and principal component analysis (PCA)
230 classified the RNA-Seq data into four groups according to genotype and nutrient condition
231 (Supplementary Fig. 6A, B). The k-means clustering analysis revealed two gene clusters for which the

232 expression was induced (cluster 2) or repressed (cluster 3) in WT/*ost2-2D* roots than in WT/WT roots
233 (Fig. 3A, B and Supplementary Table 2). Each cluster was characterized using pathway analysis;
234 cluster 2 was enriched in Gene Ontology (GO) terms associated with systemic acquired resistance
235 (SAR) and responses to fungal infection, whereas cluster 3 was enriched in the GO term "lipid X
236 metabolic process" (Fig. 3C). The expression of multiple genes encoding UDP-3-*O*-acyl N-
237 acetylglycosamine deacetylase family proteins LPXC1–5, which contribute to the biosynthesis of lipid
238 X, a precursor of lipid A-like molecules [20], was consistently repressed in WT/*ost2-2D* roots
239 (Supplementary Fig. 7A, B), although the physiological roles played by endogenous lipid A-like
240 molecules are unknown.

241

242 **4. Discussion**

243 The present study demonstrates that root-specific activation of OST2/AHA1 enhances shoot growth
244 and increases the shoot content of all the macronutrient elements and six micronutrient elements in *A.*
245 *thaliana* cultivated in nutrient-poor vermiculite (Figs. 1A and 2). The root-specific activation of
246 OST2/AHA1 also increased root weight and primary root length in plants grown in solid media (Fig.
247 1B and Supplementary Fig. 4), corresponding to root cell expansion due to apoplastic acidification,
248 i.e., acid growth [10]. Given that the availability of nutrient elements limits plant vegetative growth
249 under nutrient-poor conditions, the improvement of proton motive force and root growth could
250 facilitate nutrient uptake and shoot growth. In the present study, the concentrations of N, K, P, Mg, B,
251 and Mo in WT/WT shoots were decreased by 19%–53% when nutrient availability was reduced
252 (Supplementary Fig. 5), suggesting that the supply of these elements could limit shoot growth under
253 nutrient-poor conditions. Because the shoot content of N, K, P, Mg, B, and Mo was consistently
254 increased in WT/*ost2-2D* plants than in WT/WT plants (Fig. 2), root-specific activation of
255 OST2/AHA1 may enhance shoot growth by increasing root uptake of these elements. Interestingly,
256 root expression of the high-affinity nitrate uptake transporter *NRT2.1* and iron uptake transporter *IRT1*
257 was higher in WT/*ost2-2D* plants than in WT/WT plants under nutrient-poor conditions

258 (Supplementary Fig. 8A, B). IRT1 has broad specificity for divalent heavy metals other than Fe
259 including Mn, Zn, Co, and Cd under Fe-deficient conditions [21]. Therefore, up-regulation of *NRT2.1*
260 and *IRT1* might have contributed to increases in the shoot content of N, Mn, and Co under nutrient-
261 poor conditions (Fig. 2).

262 Our transcriptome analysis suggested that root-specific activation of OST2/AHA1 up-
263 regulates genes related to SAR and fungal infection responses in the roots (Fig. 3C). This corresponds
264 to an observation made previously that salicylic acid (SA) levels and expression of SA-responsive
265 marker genes are elevated in the leaves of *ost2-1D* mutants [9], because endogenous SA acts as a
266 signal that mediates local and systemic defense responses to pathogen infection [22]. Interestingly,
267 lowering the pH in external media *per se* is known to induce expression of genes responsive to
268 pathogens, pathogen elicitors, and SA in *A. thaliana* roots [23]. Therefore, root-specific activation of
269 OST2/AHA1 may up-regulate expression of these genes through apoplastic acidification [10].
270 In conclusion, we succeeded in increasing plant vegetative growth under nutrient-poor conditions via
271 root-specific activation of PM H^+-ATPase using a grafting strategy. Genome editing technologies are
272 applicable for substituting specific DNA sequences for a gene of interest in various plant species;
273 therefore, it may be possible to design and produce rootstocks with activated PM H^+-ATPase. Overall,
274 our study presents a novel approach to improving NUE in crops and vegetables; thus, it could
275 contribute to the implementation of low-input sustainable agriculture.

276

277 **Acknowledgments**
278 Seeds of *ost2-2D* were kindly provided by Dr. Jeffrey Leung (CNRS, France). We thank Maki Saiki
279 for ICP-MS analysis. The authors would like to thank Enago (www.enago.jp) for the English language
280 review.

281

282 **Funding**

This study was supported by a KAKENHI Grant from Japan Society for the Promotion of Science [Grant-in-Aid for Scientific Research (C) No. JP20K05771 to TH] and the Ichimura Foundation for New Technology (to TH).

Conflict of interest

The authors declare that this study was conducted in the absence of any commercial relationships that could lead to any potential conflicts of interest.

References

[1] S. Savci, An Agricultural Pollutant: Chemical Fertilizer, Int. J. Environ. Sci. Dev. 3 (2012) 77-80. https://doi.org/10.7763/IJESD.2012.V3.191.

[2] V. Kyriakou, I. Garagounis, A. Vourros, et al., An Electrochemical Haber-Bosch Process, Joule 277 (2020) 142-158. https://doi.org/10.1016/j.joule.2019.10.006.

[3] J. Cooper, R. Lombardi, D. Boardman, et al., The future distribution and production of global phosphate rock reserves, Resour. Conserv. Recycl. 57 (2011) 78–86. https://doi.org/10.1016/j.resconrec.2011.09.009.

[4] M. G. Palmgren, Plant plasma membrane H^+-ATPases: powerhouses for nutrient uptake, Annu. Rev.Plant Biol. 52 (2001) 817–845. https://doi.org/10.1146/annurev.arplant.52.1.817.

[5] M. Zhang, Y. Wang, X. Chen, et al., Plasma membrane H^+-ATPase overexpression increases rice yield via simultaneous enhancement of nutrient uptake and photosynthesis, Nat. Commun. 12 (2021) 735. https://doi.org/10.1038/s41467-021-20964-4.

[6] M. Hashimoto-Sugimoto, T. Higaki, T. Yaeno, et al., A Munc13-like protein in *Arabidopsis* mediates H^+-ATPase translocation that is essential for stomatal responses, Nat. Commun. 4 (2013) 2215. https://doi.org/10.1038/ncomms3215.

[7] F. Gévaudant, G. Duby, E. von Stedingk, et al., Expression of a Constitutively Activated Plasma Membrane H^+-ATPase Alters Plant Development and Increases Salt Tolerance, Plant Physiol. 144 (2007) 1763–1776. https://doi.org/10.1104/pp.107.103762.

[8] J. Falhof, J. T. Pedersen, A. T. Fuglsang, et al., Plasma Membrane H^+-ATPase Regulation in the Center of Plant Physiology, Mol. Plant 9 (2016) 323–337.

https://doi.org/10.1016/j.molp.2015.11.002.

[9] S. Merlot, N. Leonhardt, F. Fenzi, et al., Constitutive activation of a plasma membrane H^+-ATPase prevents abscisic acid-mediated stomatal closure, EMBO J. 26 (2007) 3216–3226. https://doi.org/10.1038/sj.emboj.7601750.

[10] E. Barbez, K. Dünser, A. Gaidora, et al., Auxin steers root cell expansion via apoplastic pH regulation in *Arabidopsis thaliana*, Proc. Natl. Acad. Sci. USA. 114 (2017) E4884–E4893. https://doi.org/10.1073/pnas.1613499114.

[11] S. D'Alessandro, Y. Mizokami, B. Légeret, et al., The Apocarotenoid β-Cyclocitric Acid Elicits Drought Tolerance in Plants, iScience 19 (2019) 461–473. https://doi.org/10.1016/j.isci.2019.08.003.

[12] J. H. Wong, M. Klejchová, S. A. Snipes, et al., SAUR proteins and PP2C.D phosphatases regulate H^+-ATPases and K^+ channels to control stomatal movements, Plant Physiol. 185 (2021) 256–273. https://doi.org/10.1093/plphys/kiaa023.

[13] K. Monden, M. Kojima, Y. Takebayashi, et al., Root-specific Reduction of Cytokinin Perception Enhances Shoot Growth in *Arabidopsis thaliana*, Plant Cell Physiol. (2022) 256–273. https://doi.org/10.1093/pcp/pcac013.

[14] T. Hachiya, T. Oya, K. Monden, et al., A cellophane-supported *Arabidopsis* culture for seamless transfer between different media is useful for studying various nitrogen responses, Soil Sci. Plant Nutr. 67 (2021) 277–282. https://doi.org/10.1080/00380768.2021.1908094.

[15] M. Notaguchi, T. Higashiyama, T. Suzuki, Identification of mRNAs that move over long distances using an RNA-Seq analysis of *Arabidopsis/Nicotiana* benthamiana heterografts, Plant Cell Physiol. 56 (2014) 311–321. https://doi.org/10.1093/pcp/pcu210.

[16] B. Langmead, C. Trapnell, M. Pop, et al., Ultrafast and memory-efficient alignment of short DNA sequences to the human genome, Genome Biol. 10 (2009) R25. https://doi.org/10.1186/gb-2009-10-3-r25.

[17] S. X. Ge, E. W. Son, R. Yao, iDEP: an integrated web application for differential expression and pathway analysis of RNA-Seq data, BMC Bioinform. 19 (2018) 534. https://doi.org/10.1186/s12859-018-2486-6.

[18] Y. Zhou, B. Zhou, L. Pache, et al., Metascape provides a biologist-oriented resource for the analysis of systems-level datasets, Nat. Commun. 10 (2019) 1523. https://doi.org/10.1038/s41467-019-09234-6.

[19] T. Hachiya, J. Inaba, M. Wakazaki, et al., Excessive ammonium assimilation by plastidic glutamine synthetase causes ammonium toxicity in *Arabidopsis thaliana*, Nat. Commun. 12

(2021) 4944. https://doi.org/10.1038/s41467-021-25238-7.

[20] C. Li, Z. Guan, D. Liu, et al., Pathway for lipid A biosynthesis in *Arabidopsis thaliana* resembling that of *Escherichia coli*, Proc. Natl. Acad. Sci. USA. 108 (2011) 11387–11392. https://doi.org/10.1073/pnas.1108840108.

[21] A. Jogawat, B. Yadav, Chhaya, et al., Metal transporters in organelles and their roles in heavy metaltransportation and sequestration mechanisms in plants, Physiol. Plant 173 (2021) 259–275. https://doi.org/10.1111/ppl.13370.

[22] D. F. Klessig, H. W. Choi, D. A. Dempsey, et al., Systemic Acquired Resistance and Salicylic Acid:Past, Present, and Future, Mol. Plant Microbe Interact. 31 (2018) 871–888. https://doi.org/10.1094/MPMI-03-18-0067-CR.

[23] I. D. A. Lager, O. Andréasson, T. L. Dunbar, et al., Changes in external pH rapidly alter plant gene expression and modulate auxin and elicitor responses, Plant Cell Environ. 33 (2010)1513–1528. https://doi.org/10.1111/j.1365-3040.2010.02161.x.

Figure legends

Fig. 1. Effects of root-specific activation of OST2/AHA1 on the growth of shoots and roots. (A) Shoot appearance, shoot fresh and dry weights, rosette diameter, and leaf blade area of the grafted plants. Grafted plants were transferred to vermiculite pots and grown for 7 days with a supply of 1/2-MS or 1/50-MS salts. All data pooled from six independent grafting experiments are presented as means ± SD (n = 43–44). (B) Root fresh and dry weights and primary and lateral root lengths of grafted plants. Grafted plants were transferred to 1/2-MS or 1/50-MS media and grown vertically for 3 days. All data pooled from four independent grafting experiments are presented as means ± SD (n = 30). WT/WT (W/W) and WT/*ost2-2D* (W/*o*) denote plants corresponding to the WT scion grafted on the WT rootstock and the WT scion grafted on the *ost2-2D* rootstock, respectively. *$P < 0.05$; ***$P < 0.001$; NS, not significant at $P > 0.05$ (unpaired two-tailed Welch's *t*-test). Scale bar: 0.5 cm.

Fig. 2. Effects of root-specific activation of OST2/AHA1 on the shoot content of nutrient elements. The shoot content of 15 nutrient elements in the grafted plants, which were transferred to vermiculite pots and grown for 7 days with a supply of 1/2-MS or 1/50-MS salts. Shoot samples

374 harvested from three (for C and N determination) and five (for determination of the other elements)
375 independent grafting experiments were subjected to element analysis. Shoots from 4 to 11 plants in
376 each experiment were pooled as one biological replicate. Data are presented as means ± SD (n = 3 or
377 5). WT/WT (W/W) and WT/*ost2-2D* (W/*o*) denote the plants corresponding to the WT scion grafted
378 on the WT rootstock and the WT scion grafted on the *ost2-2D* rootstock, respectively. *$P < 0.05$;
379 **$P < 0.01$; NS† $P < 0.1$; NS, not significant at $P > 0.05$ (unpaired two-tailed Welch's *t*-test).
380
381 **Fig. 3. Effects of root-specific activation of OST2/AHA1 on the root transcriptome.** (A) Heat map
382 from k-means clustering, (B) violin plots of normalized transcript levels in clusters 2 and 3, and (C)
383 pathway analyses of the genes in clusters 2 and 3. Grafted plants were transferred to 1/2-MS or 1/50-
384 MS media and grown horizontally for 7 days. Root samples harvested from two independent grafting
385 experiments were subjected to RNA-Seq analysis. Roots from four plants in each experiment were
386 pooled as one biological replicate. Genes for which the standard deviation was ranked in the top 2000
387 were used for k-means clustering with four clusters, which included 769, 288, 219, and 724 genes
388 (clusters 1–4), respectively. Purple and green represent higher and lower expressions, respectively.
389 Information about genes included in each cluster is provided in Supplementary Table 3. Pathway
390 analyses were performed using the obtained clusters 2 and 3, and significantly enriched terms are
391 shown. WT/WT (W/W) and WT/*ost2-2D* (W/*o*) denote plants corresponding to the WT scion grafted
392 on the WT rootstock and the WT scion grafted on the *ost2-2D* rootstock, respectively.

Figure 1

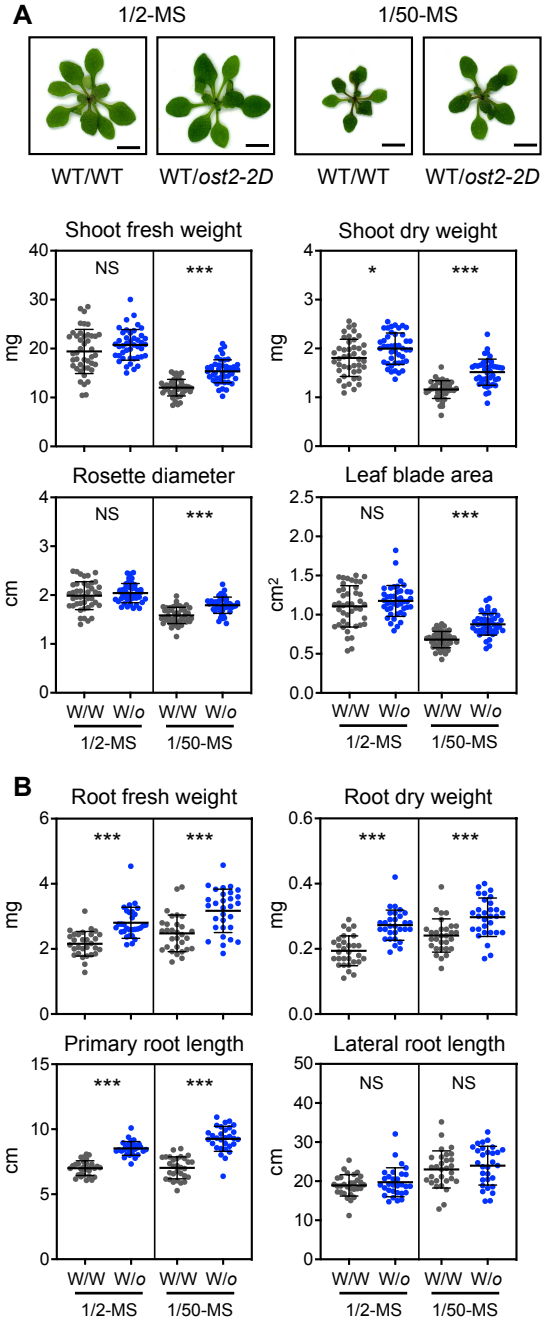
A
1/2-MS
1/50-MS
WT/WT
WT/ost2-2D
WT/WT
WT/ost2-2D
Shoot fresh weight
Shoot dry weight
Rosette diameter
Leaf blade area
mg
cm
cm2
NS
***
*
W/W
W/o
1/2-MS
1/50-MS
B
Root fresh weight
Root dry weight
Primary root length
Lateral root length

Figure 2

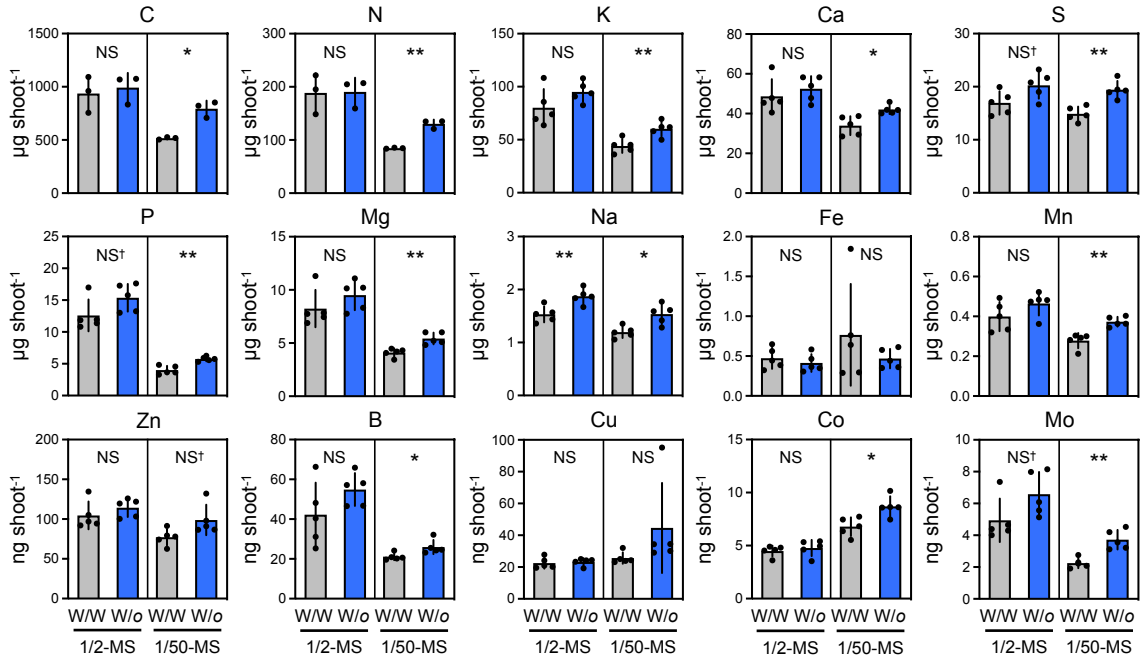
C
N
K
Ca
S
P
Mg
Na
Fe
Mn
Zn
B
Cu
Co
Mo
μg shoot-1
ng shoot-1
NS
NS†
*
**
W/W
W/o
1/2-MS
1/50-MS

Figure 3

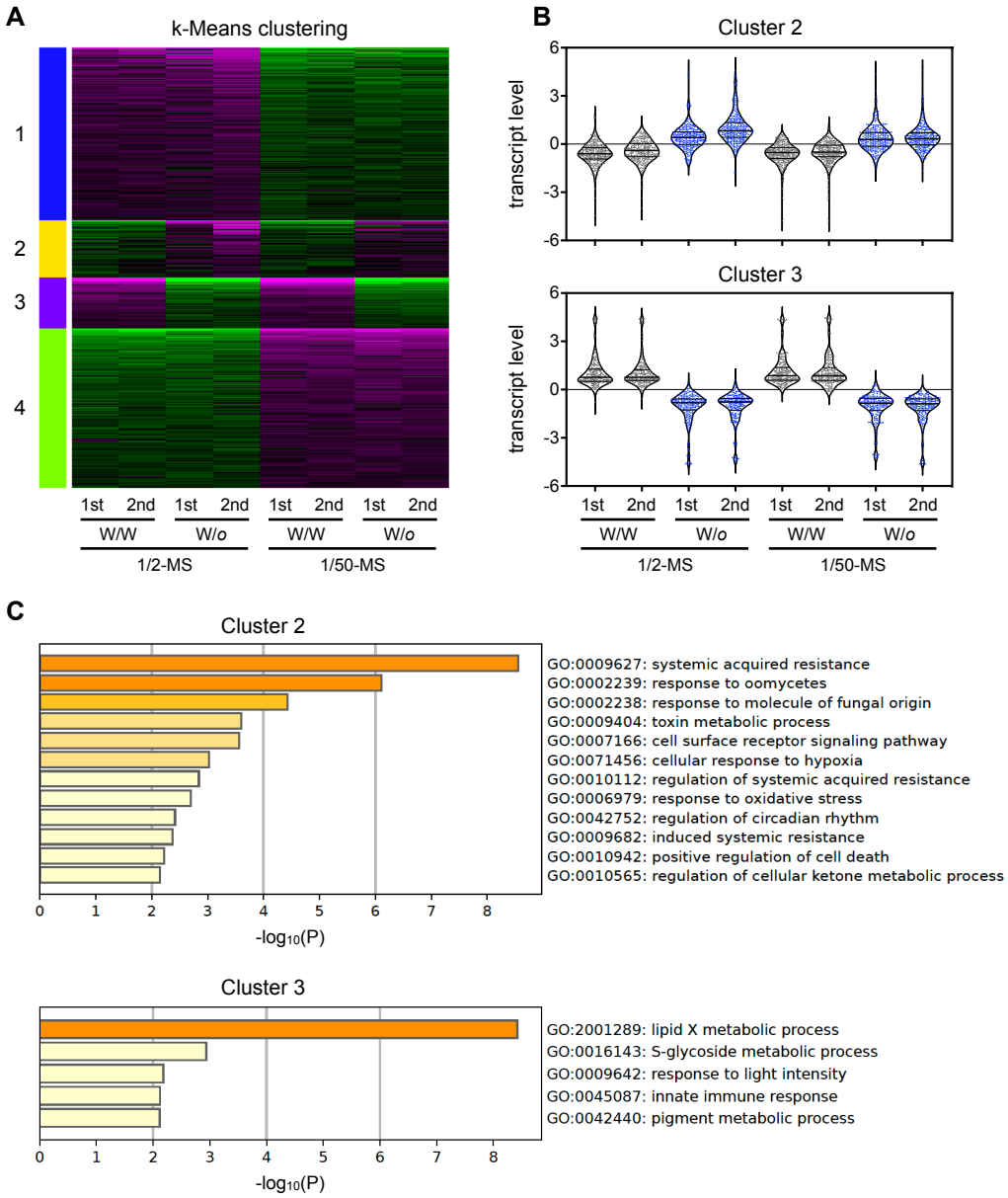
A
k-Means clustering
1
2
3
4
1st 2nd 1st 2nd 1st 2nd 1st 2nd
W/W W/o W/W W/o
1/2-MS 1/50-MS
B
Cluster 2
transcript level
6
3
0
-3
-6
Cluster 3
1st 2nd 1st 2nd 1st 2nd 1st 2nd
W/W W/o W/W W/o
1/2-MS 1/50-MS
C
Cluster 2
GO:0009627: systemic acquired resistance
GO:0002239: response to oomycetes
GO:0002238: response to molecule of fungal origin
GO:0009404: toxin metabolic process
GO:0007166: cell surface receptor signaling pathway
GO:0071456: cellular response to hypoxia
GO:0010112: regulation of systemic acquired resistance
GO:0006979: response to oxidative stress
GO:0042752: regulation of circadian rhythm
GO:0009682: induced systemic resistance
GO:0010942: positive regulation of cell death
GO:0010565: regulation of cellular ketone metabolic process
0 1 2 3 4 5 6 7 8
-log10(P)
Cluster 3
GO:2001289: lipid X metabolic process
GO:0016143: S-glycoside metabolic process
GO:0009642: response to light intensity
GO:0045087: innate immune response
GO:0042440: pigment metabolic process
0 1 2 3 4 5 6 7 8
-log10(P)